Carbohydrate Polymers 90 (2012) 1732–1738

Contents lists available at SciVerse ScienceDirect

Carbohydrate Polymers

journal homepage: www.elsevier.com/locate/carbpol

Rheological properties of suspensions containing cross-linked starch nanoparticles prepared by spray and vacuum freeze drying methods

Ai-min Shi[a,1], Dong Li[a,1], Li-jun Wang[b,*], Benu Adhikari[c]

[a] College of Engineering, China Agricultural University, P.O. Box 50, 17 Qinghua Donglu, Beijing 100083, China
[b] College of Food Science and Nutritional Engineering, China Agricultural University, Beijing, China
[c] School of Health Sciences, University of Ballarat, VIC 3353, Australia

ARTICLE INFO

Article history:
Received 15 April 2012
Received in revised form 10 June 2012
Accepted 24 July 2012
Available online 31 July 2012

Keywords:
Rheological behavior
Starch nanoparticles
Spray drying
Vacuum freeze drying
Suspensions

ABSTRACT

The rheological behavior of suspensions containing vacuum freeze dried and spray dried starch nanoparticles was investigated to explore the effect of these two drying methods in producing starch nanoparticles which were synthesized using high pressure homogenization and mini-emulsion cross-linking technique. Suspensions containing 10% (w/w) spray dried and vacuum freeze dried nanoparticles were prepared. The continuous shear viscosity tests, temperature sweep tests, the frequency sweep and creep-recovery tests were carried out, respectively. The suspensions containing vacuum freeze dried nanoparticles showed higher apparent viscosity within shear rate range (0.1–100 s^{-1}) and temperature range (25–90 °C). The suspensions containing vacuum freeze dried nanoparticles were found to have more shear thinning and less thixotropic behavior compared to those containing spray dried nanoparticles. In addition, the suspensions containing vacuum freeze dried particles had stronger elastic structure. However, the suspensions containing spray dried nanoparticles had more stiffness and greater tendency to recover from the deformation.

1. Introduction

Starch nanoparticles (particle size 1–1000 nm) comprising starch molecules and various cross-linkers are new class of biomaterials (Rodrigues & Emeje, 2012; Simi & Emilia Abraham, 2007). They have excellent mechanical and inherent functional properties such as low/non toxicity, low immunogenicity and good biocompatibility. Because of this reason, these starch nanoparticles have drawn considerable attention in food (Arora & Padua, 2010), medicine (Santander-Ortega et al., 2010), textile (Vigneshwaran et al., 2006), and biotechnology fields (Xiao et al., 2005). These starch nanoparticles have been regarded as highly valuable for their potential application as drug carrier materials in pharmaceutical industry (Jain, Khar, Ahmed, & Diwan, 2008; Kumari & Rani, 2011; Malam, Lim, & Seifalian, 2011; Mohanraj & Chen, 2006).

Physical methods such as precipitation (Ma, Jian, Chang, & Yu, 2008) and microfluidization (Liu, Wu, Chen, & Chang, 2009) can produce these starch nanoparticles. Similarly chemical methods such as emulsion polymerization (Wang, Liu, & Pope, 2003) and emulsion cross-linking (Jain et al., 2008) can be used to produce these nanoparticles. Among these methods, emulsion cross-linking has been applied more commonly to manufacture various starch nanoparticles (Agnihotri, Mallikarjuna, & Aminabhavi, 2004; Bodnar, Hartmann, & Borbely, 2006). The emulsion cross-linking method has become the method of choice because it is easy to carry out and the yield of the nanoparticles is fairly high. When high pressure homogenizer is applied to produce the emulsions, this method is capable of reducing amount of surfactants used, lowering the particle size with ease, and increasing the productivity (Liu et al., 2009; Mcclements, Decker, & Weiss, 2007).

When the nanoparticles are produced, it is necessary to remove the solvent, especially water by drying. The drying step is necessary to extend the storage life of the starch nanoparticles and to reduce the volume/weight of the final product. So far, spray drying and vacuum freeze drying are the two most commonly used methods for removing the water in the production of nanoparticles (Jain et al., 2008; Patil, Dandekar, Patravale, & Thorat, 2010). The particle temperature (during drying) and the rate of water removal are quite different in these two drying systems. Because of these reasons, the final particles produced by using these two drying systems are quite different, especially in appearance, particle size, degree of crystallization, and re-dispersibility. Among these properties, re-dispersibility of particles can have remarkable influence or impact on their application (Kho & Hadinoto, 2010). The rheological properties can be excellent indicators of the re-dispersing behavior of

---

* Corresponding author. Tel.: +86 10 62737351; fax: +86 10 62737351.
E-mail address: wlj@cau.edu.cn (L.-j. Wang).
[1] These authors contributed equally to this work.

0144-8617/$ – see front matter © 2012 Elsevier Ltd. All rights reserved.
http://dx.doi.org/10.1016/j.carbpol.2012.07.059

suspensions containing these starch nanoparticles (Kimura et al., 2011).

The rheological properties, which include the continuous shear viscosity and storage or loss modulus, vary with shear rate, temperature, frequency and time. The rheological properties of suspensions containing nanoparticles are investigated and reported. For example, the rheological features of suspensions containing chitosan–sodium tripolyphosphate nanoparticles (Li & Huang, 2012), iron nanoparticles (Borin, Zubarev, Chirikov, Müller, & Odenbach, 2011), cell-wall particle (Day, Xu, Øiseth, Lundin, & Hemar, 2010) and silica nanoparticles (Triebel & Münstedt, 2011) have been reported. However, to the best of our knowledge, there are no publications reporting the effect of drying methods (used to produce nanoparticles) on the rheological properties of suspension containing starch nanoparticles. Therefore, the objective of this study was to investigate the effect of two drying methods (vacuum freeze drying and spray drying) on the rheological properties of suspensions containing these starch nanoparticles. The continuous shear viscosity tests are carried out to determine the effect of shear rate and temperature on apparent viscosity of the suspensions. The dynamic rheological tests are carried out to investigate the effect of frequency on the elastic and loss modulus and phase angle. The creep recovery test is carried out to determine the extent of recovery (from deformation) of the suspensions from applied stress. The Cross model is used to represent the shear dependent viscosity while the Power Law type equations are used to represent the frequency dependence of storage and loss modulus. The creep-recovery data are modeled using Burger's model which contains Maxwell and Kelvin models in series.

2. Materials and methods

2.1. Materials

Soluble starch was purchased from Beijing Aoboxing Biological Technique Company (Beijing, China). Sodium chloride, sodium hydroxide, cyclohexane, acetone and acetic acid were provided by Beijing Chemical Company (Beijing, China). Tween-80 and Span-80 were purchased from Tianjing Fuchen Chemical Company (Tianjing, China). Sodium trimetaphosphate (STMP) was obtained from Tianjing Dengfeng Chemical Company (Tianjing, China). All of these reagents were of analytical grade and used without further purification. Deionized water was used throughout the work.

2.2. Preparation of starch nanoparticles

The method used to prepare the starch nanoparticles is based on the emulsion cross-linking technology using a high pressure homogenizer and is reported in our previous work (Shi, Li, Wang, Li, & Adhikari, 2011).

After twice washing with acetone, starch nanoparticles were dispersed into 100 mL deionized water for further drying.

2.3. Drying methods

The dried starch nanoparticles were prepared using spray drying and vacuum freeze drying methods as described below.

2.3.1. Spray drying method

A bench-top spray dryer (GPW120-II, Shandong Tianli Drying Equipment Co., Ltd., Shandong, China) with 500 mL/h evaporation capacity was used throughout the spray drying trials. The atomization of the droplet was accomplished using a 0.7 mm two-fluid nozzle and compressed air was used as atomizing medium. The flow rate of the compressed air was 10 L/min and its pressure was maintained at 608 kPa. The feed flow rate and inlet temperature were set at 5.4 mL/min and 100 °C, respectively. The powders were collected at the cyclone and finally transferred to zip-lock bags. These spray dried starch nanoparticles were stored in desiccator containing dried allochroic silicagel under 25 °C.

2.3.2. Freeze drying method

A laboratory-scale vacuum freeze dryer (LGJ-18, Sihuan, China) was used to dry the starch nanoparticles. The sample dishes ($0.1\,\text{m}^2 \times 3\,\text{cm}$) containing the suspension ($0.1\,\text{m}^2 \times 1\,\text{cm}$) were placed in the cold trap of the vacuum freeze dryer (−60 °C) for 5 h to ensure complete freezing of the sample. Subsequently, the frozen samples were placed in drying chamber and then the chamber was evacuated (<100 Pa). The temperature of frozen samples was varied from −30 °C to 45 °C step by step in the 28 h-long drying period (1 h each at −30 °C, −25 °C, −20 °C, −15 °C, −10 °C, −5 °C; 2 h each at 0 °C, 5 °C, 10 °C, 15 °C, 20 °C, 25 °C, 30 °C, 35 °C, 40 °C and finally 4 h each at 45 °C). The vacuum freeze dried starch nanoparticles were stored in the same desiccator in which spray dried samples were stored.

2.4. Suspension preparation

According to our previous research, the moisture content of spray dried sample was 9.6% (w/w, dry base) and that of the vacuum-freeze dried sample was 8.15% (w/w, dry base). For rheological tests, dried starch nanoparticles were added into deionized water and stirred using a magnetic stirrer (300 rpm) for 30 min at 25 °C to make the 10% (w/w, wet basis) suspensions.

2.5. Rheological tests

Rheological measurements were performed using AR2000ex rheometer (TA Instruments Ltd., New Castle, DE). The temperature was controlled and adjusted by the Peltier Plate system which contained a platinum resistance thermometer (PRT) sensor positioned in the middle of the lower sample plate and ensured accurate measurement and control of sample temperature. A thin layer of silicone oil was applied on the surface of the samples in order to prevent evaporation. The linear viscoelastic region was determined for each sample through strain sweeps at 1 Hz (data not shown). Storage modulus G', loss modulus G'', and δ of starch nanoparticles suspensions were determined within the linear viscoelastic region. An equilibration time of 2 min was maintained before each measurement.

2.5.1. Continuous shear viscosity measurements

The continuous shear tests were performed at 25 °C over the shear rate range of $0.1–100\,\text{s}^{-1}$ to measure the apparent viscosity. A parallel plate (40 mm diameter, 1 mm gap) was chosen for the continuous shear viscosity measurements.

2.5.2. Flow curves measurements

The flow curves of the suspensions containing starch nanoparticles (produced using both the vacuum freeze and spray drying methods) were measured at 25 °C with the shear rate range increasing from $0.1\,\text{s}^{-1}$ to $100\,\text{s}^{-1}$, then decreasing from $100\,\text{s}^{-1}$ to $0.1\,\text{s}^{-1}$. A parallel plate (40 mm diameter, 1 mm gap) was chosen for these flow curve measurements.

2.5.3. Temperature ramp measurements

The temperature ramp measurements were carried out using a shear rate of $5\,\text{s}^{-1}$ and the test temperature was increased from 25 °C to 90 °C at a heating rate of 2 °C/min. The test temperature was maintained at 90 °C for 3 min. Finally the test temperature was lowered to 25 °C at a cooling rate of 2 °C/min. The sample was held at 25 °C for 5 min. A parallel plate (40 mm diameter, 1 mm gap) was chosen for the temperature ramp measurements.

2.5.4. *Frequency sweep measurements*

The frequency sweep tests were performed at 25 °C over the angular frequency range of 0.1–10 rad/s. The oscillating stress for the frequency sweep measurements was selected as 0.7958 Pa according to the strain sweep results (data not shown) in order to confine within the linear viscoelastic region for all samples. A parallel plate geometry (40 mm diameter, 1 mm gap) was chosen for these frequency sweep measurements.

2.5.5. *Creep-recovery measurements*

Creep-recovery experiments were carried out using a shear stress of 7.958 mPa at 25 °C. The variation in shear strain in response to the applied stress was measured over a period of 2 min. The stress was subsequently removed, and the changes in strain were recorded for a further period of 2 min. A parallel plate (40 mm diameter, 1 mm gap) was chosen for these creep-recovery measurements.

2.6. *Statistical analysis*

All of these rheological measurements were carried out in triplicate. The experimental rheological data were obtained directly from the TA Rheology Advantage Data Analysis software V 5.4.7 (TA Instruments Ltd., Crawley, UK). The average of the three runs was reported as the measured value with standard deviation.

Duncan's multiple comparison method was used to determine the significant effect of different drying processes on the rheological properties of the suspensions containing vacuum freeze and spray dried starch nanoparticles. A confidence level was set at $p < 0.05$ and the SAS software (SAS Institute Inc., Cary, NC, USA) was used in these statistical analyses. The apparent viscosity data were modeled according to Cross model which is frequently used for suspensions, dispersions, polymer solutions or melts and the creep data were modeled according to Berger's model, using the non-linear regression feature in SPSS 13.0 (SPSS Inc., Chicago, USA).

3. Results and discussion

3.1. *Continuous shear viscosity properties*

In order to describe the variation in the flow properties of suspension containing cross-linked starch nanoparticles (obtained by spray and freeze drying as described in Section 2.3) under continuous shear, the Cross model (Eq. (1)) is used (Susan-Resiga, Bica, & Vékás, 2010).

$$\eta = \eta_\infty + \frac{\eta_0 - \eta_\infty}{1 + (C\dot{\gamma})^m} \tag{1}$$

Here η is the apparent viscosity (Pa s), η_∞ is the viscosity at infinite shear rate (Pa s), η_0 is the viscosity at zero shear rate, c is the consistency (s), $\dot{\gamma}$ is the shear rate (s^{-1}), and m is the flow behavior index (dimensionless).

The predicted apparent viscosity values are obtained by fitting the experimental flow curves to Cross model. The flow curves of the suspensions (10%, w/w) of starch nanoparticles dried by both the spray and freeze drying methods are shown in Fig. 1. As we can see from this figure, the apparent viscosity of all the samples decreases with the increase in the shear rate. Specifically, for suspension containing spray dried starch nanoparticles, the viscosity changed from 6.88 to 0.14 Pa s with shear rate varying from 0.1 to 100 s^{-1} while for suspension containing vacuum-freeze dried starch nanoparticles, the viscosity changed from 9.53 to 0.17 Pa s. And from Table 1 the flow behavior index (m) in Eq. (1) was all over zero and the Cross model, a typical shear thinning model, fitted the flow curves well with $R^2 > 0.995$. These illustrate that the suspensions of the starch nanoparticles exhibit shear-shining behavior. It can further be seen from Fig. 1 that the suspension containing nanoparticles dried using vacuum freeze drying shows higher apparent viscosity than the suspension containing spray dried particles throughout the shear rate range. This indicates that the characteristics of the starch nanoparticles obtained from these two drying methods are different. As reported previously and from Fig. 2, because of the

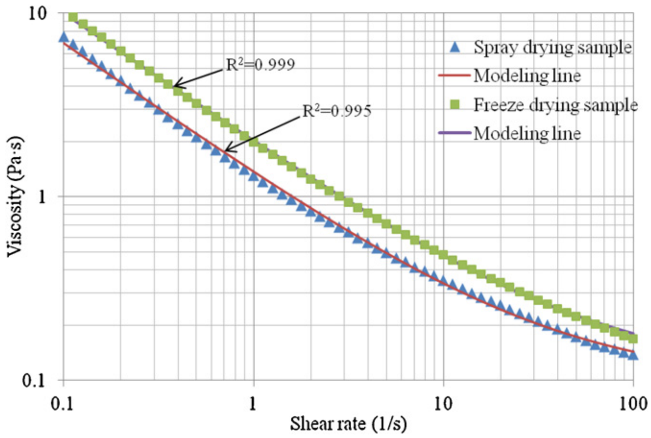

Fig. 1. Effect of the drying methods on the apparent viscosities of 10% (w/w) starch nanoparticles suspension.

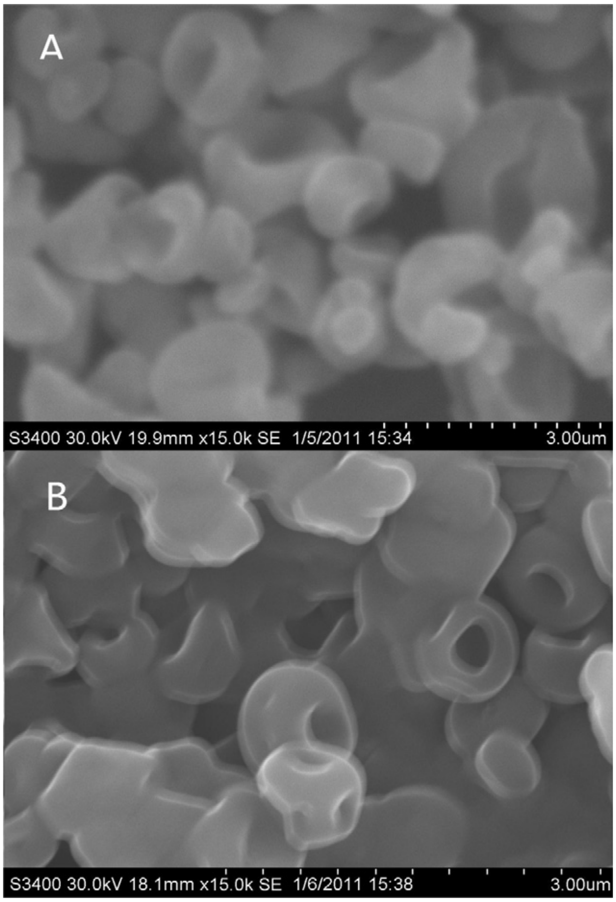

Fig. 2. The SEM images of starch nanoparticles prepared through different drying methods: (A) represents spray dried sample and (B) represents vacuum freeze dried sample.

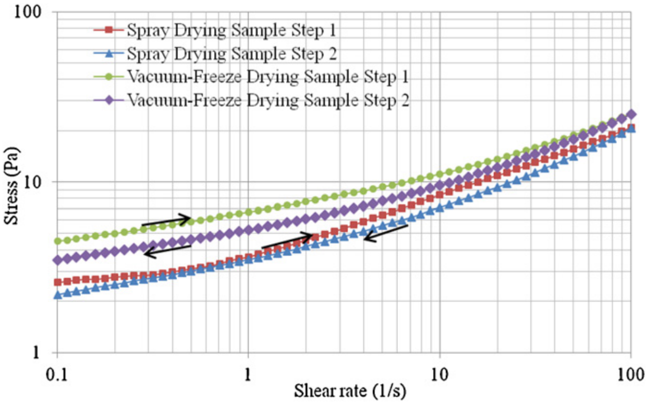

Fig. 3. Flow curves of spray and vacuum freeze dried starch nanoparticles suspensions at solid concentration of 10% (w/w) at 25 °C.

aggregation and swelling, the particles produced through spray drying had higher particle size (1000–2000 nm) and lower particle number density (per unit volume of suspension) than the particles produced through vacuum freeze drying (700–900 nm) (Shi, Wang, Li, & Adhikari, 2012). Due to much higher particle number density the suspensions containing vacuum freeze dried particles are expected to have greater hydrodynamic interactions at the same shear rate which resulted into higher apparent viscosity (Chevalier, Tillement, & Ayela1, 2009). Furthermore, it was observed during the experiments that the spray dried particles resisted dispersion and more agglomeration occurred compared to the vacuum freeze dried particles. The freeze dried mass easily turned into individual particles at very low shear or even during gentle manual handling. The consistency or visual appearance of both the spray dried and vacuum freeze dried suspensions was very close at higher shear rates which corroborates with fact that the measured viscosity values of both the suspensions were very close at the shear rate of $100\,s^{-1}$.

The parameters obtained by fitting Cross model to experimental data are presented in Table 1. This model shows that the viscosity of the suspension containing spray dried particles at zero shear rate is 2.161×10^5 Pa s while the viscosity of the suspension containing vacuum freeze dried particles is 4.119×10^5 Pa s. Interestingly, the infinite-rate viscosity values of the suspensions containing spray and vacuum freeze dried particles are 0.116 Pa s and 0.109 Pa s, respectively which are statistically insignificant ($p > 0.05$). This illustrates that the apparent viscosity of starch suspensions containing nanoparticles varies with variation in shear rate and ultimately these two suspensions display the similar viscosity because of the same mass concentration of starch nanoparticles.

It can also be seen from Table 1 that the *c* and *m* values of suspension containing vacuum freeze dried particles are higher than those of suspension containing spray dried particles. This result shows that suspensions containing vacuum freeze dried starch nanoparticles undergo higher shear thinning than the suspensions containing spray dried particles.

3.2. Shear stress–shear rate rheograms

Fig. 3 shows the shear stress–shear rate rheograms of suspension containing starch nanoparticles obtained from both drying methods. The rheograms of shear stress *versus* shear rate show the non-Newtonian shear thinning characteristics of these suspensions (Maroda et al., 2011; Rodríguez-Marín, Núñez-Santiago, Wang, & Bello-Pé rez, 2010). It can be seen from this figure that both the suspensions display hysteresis between the shear increasing (up curve, $0.1–100\,s^{-1}$) and shear decreasing (down curve,

Table 1
Model parameters of apparent viscosity and elastic modulus of 10% (w/w)starch nanoparticles suspension prepared by different drying methods.

Drying methods	Cross model parameters of apparent viscosity[a]					Power Law parameters of G′, and G″ [a]					
	η_0 (10^5 Pa s)	η_∞ (Pa s)	c (10^6 s)	m	R^2	K' (Pa s^n)	n'	R^2	K'' (Pa s^n)	n''	R^2
Spray drying	2.161 ± 0.342a	0.116 ± 0.004a	1.435 ± 0.428a	0.759 ± 0.003a	0.995	11.298 ± 0.010a	0.095 ± 0.001a	0.998	2.500 ± 0.035a	0.181 ± 0.010a	0.897
Vacuum-freeze drying	4.119 ± 0.490b	0.109 ± 0.002b	7.552 ± 0.465b	0.822 ± 0.001b	0.999	16.051 ± 0.010b	0.090 ± 0.001b	0.999	2.601 ± 0.039b	0.233 ± 0.009b	0.939

Values in a column with different letters were significantly different ($p < 0.05$).

[a] Values represent the mean ± standard deviation of triplicate tests.

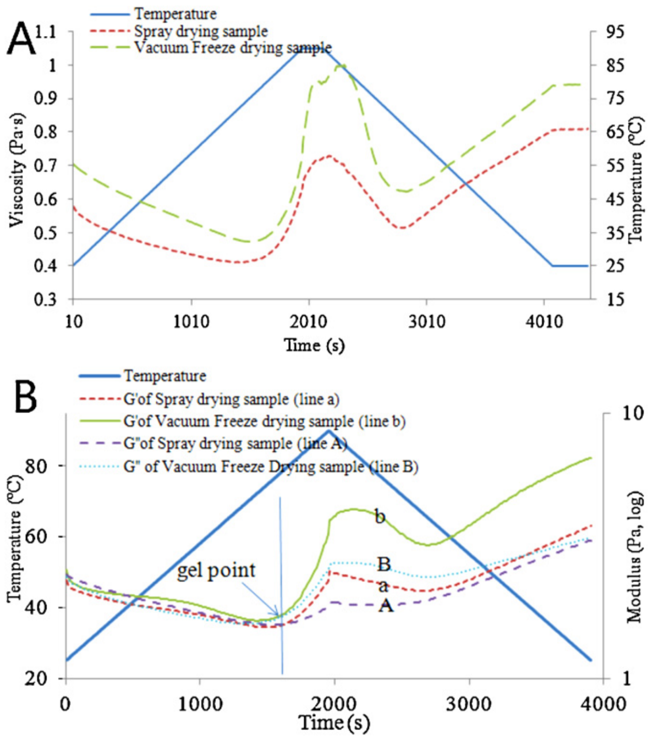

Fig. 4. The variation of apparent viscosity and viscoelastic modulus with temperature of 10% (w/w) starch nanoparticles suspension containing starch nanoparticles obtained from spray drying and vacuum freeze drying.

100–0.1 s^{-1}) curves. The hysteresis might have been resulted from the swelling of starch nanoparticles due to interaction of OH-groups of starch when they form hydrogen bonds with water molecules in suspension. Fig. 3 further shows that the shear stress of the suspensions containing vacuum freeze dried particles is always higher compared to that of the suspensions containing spray dried nanoparticles within the entire shear rates tested. The data presented in Fig. 3 corroborate the apparent viscosity data presented in Fig. 2 that the apparent viscosity values of suspension containing vacuum freeze dried particles were always higher than the those suspensions containing spray dried particles within the entire shear rate tested.

A careful observation of up curve and down curve of these two types of suspensions reveals that the hysteresis loop areas (Pa s^{-1}) (between up and down curves at chosen shear rate) of suspension containing vacuum freeze dried sample is 99.88 Pa s^{-1} and that of suspension containing spray dried samples is 117.97 Pa s^{-1}. When a suspension traverses through an increasing and decreasing shear loop/cycle as describe in Fig. 3, it takes time for internally perturbed structure to recover. When this shear cycle completes, it makes a homodeisterse of starch nanoparticles in the suspension. This is the reason why the suspension's viscosity at down cycle was lower than that in up cycle, generating a fusiform loop whose area is a measure of thixotropy (Cai et al., 2011). Thus, suspension containing vacuum freeze dried sample has less thixotropic behavior than that containing spray dried sample.

3.3. Temperature sweep properties

The rheograms of suspensions containing starch nanoparticles prepared from both the drying methods are shown in Fig. 4(A). These two suspensions show similar trend but different magnitude of viscosity as a function of temperature. Specifically, in the first 1500 s, when the temperature was below 70 °C, the viscosity of both the suspensions decreased in similar fashion and both the suspensions exhibited shear thinning trend. This may be due to the fact that the increase in the thermal energy provided additional kinetic energy to starch dispersions or starch molecules which resulted into lower lowering of the shear viscosity with increase in suspension temperature. Furthermore, declustering/break up of particle aggregation can also be possible reason for the decrease in shear viscosity when the thermal energy (temperature) is allowed to increase at the same time when the shearing action is maintained.

However, when the temperature increased above 70 °C, it led to a large increase in viscosity of both the suspensions. Heating might have induced disruption of intra and inter molecular hydrogen bonds between starch chains in starch nanoparticles. These effects of heating facilitate the swelling of starch nanoparticles (Chung, Min, Kim, & Lim, 2007) which is commonly known as gelatinization (Fig. 4(B)). It is then reasonable to expect that the viscosity of suspension containing these fully swelled starch nanoparticles is remarkably higher because of higher hydrodynamic size of the swelled nanoparticles. Meanwhile, when the temperature dropped to 70 °C, the viscosity of suspension containing starch nanoparticles also reduced to a normal value. This recovery or reversibility in viscosity indicates that the main structure of most starch nanoparticles has not been irreversibly destroyed (Fig. 4(A)). The small disparity (or difference) in viscosity values at the beginning of heating cycle and at the end of the heating cycle might be due to the residual heat energy still remaining in the dispersion and as a consequence the hydrodynamic radius of the starch nanoparticles being lager compared to the size at the start of the heating cycle. Between these two types of suspensions, the one containing vacuum freeze dried particles always displayed higher viscosity than the suspension containing spray dried particles within the entire temperature range. This difference can be explained from the characteristic difference in the nanoparticles produced from these two types of drying methods as mentioned Section 3.1.

3.4. Frequency sweep properties

Fig. 5 shows the variation of storage modulus (G'), loss modulus (G''), and loss angle (δ) as a function of frequency at 25 °C for 10% (w/w) suspensions containing the two different starch nanoparticles. It can be seen from this figure that the moduli (G' and G'') of these two dispersions increase with the increase in the angular frequency. The values of the phase angle (δ) remained almost constant at 10°, which illustrates that the storage modulus is higher than the loss modulus in these two dispersions throughout the frequency range.

The G' of suspension containing vacuum freeze dried starch nanoparticles is always higher than that of suspension containing spray dried nanoparticles both of which follow similar increasing trend when the angular frequency increased. The G'' values of both the vacuum freeze dried and spray dried nanoparticles suspensions is the same at low frequency (0.1–1 rad/s). As can be seen from Fig. 5, when the angular frequency increases from 1 to 10 rad/s, the G'' of suspension containing vacuum freeze dried sample is slightly higher than that of suspension containing spray dried sample. The δ values of the suspensions containing vacuum freeze dried particles are higher than those of dispersions containing spray dried particles, similar to the trend seen in G' values.

The frequency dependence of G' and G'' of suspension containing starch nanoparticles can be represented by Power Law type equations, represented by Eqs. (2) and (3) below (Wang, Wang, Li, Xue, & Mao, 2009).

$$G' = K' \cdot \omega^{n'} \tag{2}$$

$$G'' = K'' \cdot \omega^{n''} \tag{3}$$

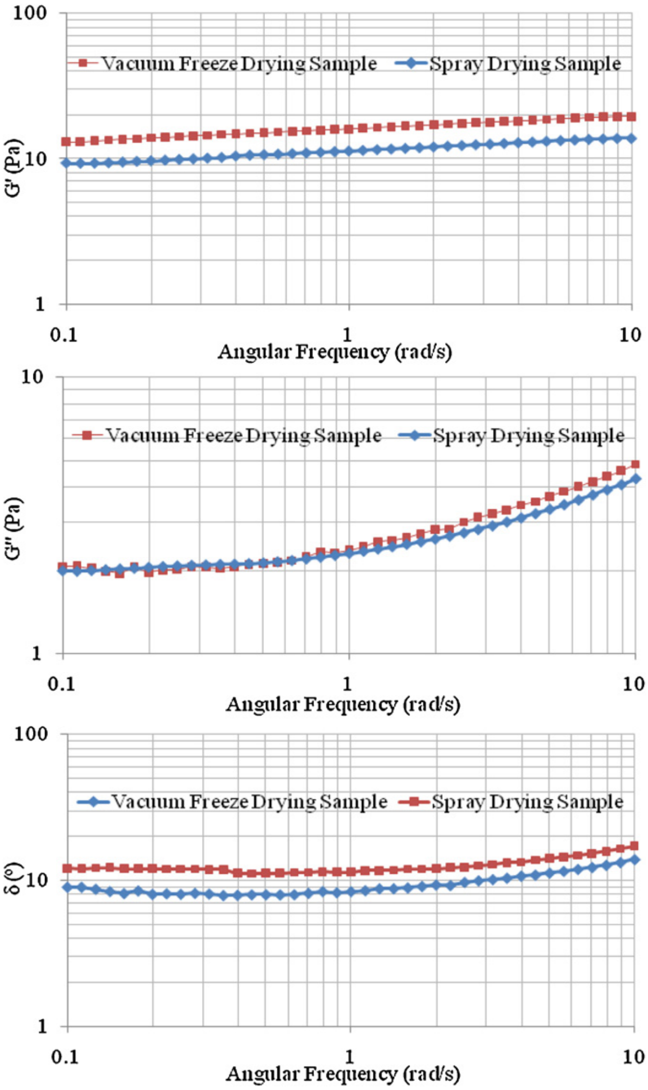

Fig. 5. Frequency dependence of 10% (w/w) starch nanoparticles suspension prepared by different drying methods.

where K' and K'' are constants and reflect the elastic and viscous properties, respectively. n' and n'' are referred to as the frequency exponents and ω is the angular frequency.

The Power Law parameters of G' and G'' for these two suspensions are presented in Table 1. The G' and G'' obeyed the Power Law equations well with the linear regression coefficients (R^2) being higher than 0.897. The K' values (11.298 Pa s^n, 16.051 Pa s^n) of these two suspensions is much higher than the K'' values (2.500 Pa s^n, 2.601 Pa s^n), indicating that the suspensions containing starch nanoparticles are more elastic than viscous. Meanwhile, the K' and K'' values of suspensions containing vacuum freeze dried sample are slightly higher than those of dispersions containing spray dried sample. These findings indicate that the vacuum freeze dried nanoparticles can lead to the formation of more elastic structure in the suspensions compared to when spray dried particles are used. The n' and n'' values of both the vacuum freeze and spray dried particles are very close to each other indicating that these two suspensions have similar frequency sensitivity.

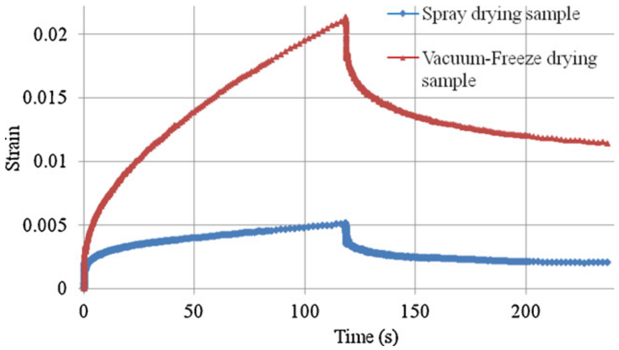

Fig. 6. Creep-recovery behaviors of 10% (w/w) starch nanoparticles suspension prepared by different drying methods.

3.5. *Creep-recovery measurements*

The creep-recovery behavior of suspension containing starch nanoparticles obtained from both the drying methods is presented in Fig. 6. The suspension containing the vacuum freeze dried particles deformed to a greater extent during the creep test compared to the suspension containing spray dried particles. Both the suspensions showed some degree of recovery from deformation when the stress is lifted.

The creep behavior can be described using Burger's model, which is composed of a Maxwell model and a Kelvin model arranged in series (Jia, Peng, Gong, & Zhang, 2011):

$$\varepsilon = \frac{\sigma_0}{E_M} + \frac{\sigma_0}{E_K}(1 - e^{-t/\tau}) + \frac{\sigma_0}{\eta_M} \cdot t \qquad (4)$$

$$\tau = \frac{\eta_K}{E_K} \qquad (5)$$

where t represents the time after loading, E_M and η_M are the modulus and viscosity of the Maxwell spring and dashpot, respectively. Similarly, E_K and η_K are the modulus and viscosity of the Kelvin spring and dashpot, respectively; $\tau = \eta_K / E_K$ is the retardation time taken to produce 63.2% or $(1 - e^{-1})$ of the total deformation in the Kelvin unit. The parameters E_M, E_K, η_M, and τ can be obtained from fitting the experimental data to the Eqs. (4) and (5) with SPSS software.

The values of above mentioned four parameters for these two types of suspensions are summarized in Table 2. As can be seen from this table, the suspension containing spray dried starch nanoparticles has higher E_M, higher E_K, lower τ, and higher η_M than those suspensions containing vacuum freeze dried starch nanoparticles. The parameter E_M is associated with the Maxwell spring establishes instantaneous creep strain that would be recovered after removal of the stress (Jia et al., 2011). This analysis shows that the suspension containing spray dried nanoparticles has higher propensity to recover compared to the suspension containing vacuum freeze dried particles. The retardant elasticity E_K is related

Table 2
Parameters of Berger's model of starch nanoparticles suspension and recovery percentage in creep-recovery test of 10% (w/w) starch nanoparticles suspension.[a]

Drying methods	E_M (Pa)	E_K (Pa)	τ (s)	η_M (Pa s)	R^2	Recovery (%)
Spray drying	17.891 ± 1.704a	3.968 ± 0.093a	0.582 ± 0.037a	292.980 ± 7.133a	0.940	59.7
Vacuum-freeze drying	8.680 ± 0.638b	1.506 ± 0.028b	2.290 ± 0.121b	56.407 ± 0.685b	0.985	45.8

Values in a column with different letters were significantly different ($p < 0.05$).
[a] Values represent the mean ± standard deviation of triplicate tests.

to the stiffness of polymer chains (chemical bonds) and η_K indicates the viscosity of the Kelvin–Voigt unit. The ratio of η_K/E_K is the relaxation time τ (Jia et al., 2011). This analysis suggests that spray dried starch nanoparticles display more stiffness compared to the vacuum freeze dried starch nanoparticles. This analysis also indicates that the relaxation time of spray dried starch nanoparticles is shorter than that of vacuum freeze dried particles. The increase in the parameter η_M leads to the decrease in the permanent deformation. The decrease in the permanent deformation ultimately affects the recovery rate of the suspension (Jia et al., 2011). This analysis further shows that the spray dried starch nanoparticles have less irrecoverable creep deformation than the vacuum freeze dried nanoparticles.

4. Conclusions

The rheological characteristics of suspensions containing vacuum freeze dried and spray dried starch nanoparticles was investigated. The suspensions containing vacuum freeze dried nanoparticles showed higher apparent viscosity compared to the suspensions containing spray dried nanoparticles within 0.1–100 s^{-1} shear rate and 25–90 °C temperature range. The suspensions containing vacuum freeze dried particles had greater propensity to undergo shear thinning compared to the suspensions containing spray dried nanoparticles. The stress–strain rheograms of both the suspensions exhibited hysteresis as a function of increasing and decreasing shear rates indicating that these suspensions were thixotropic in nature. The suspension containing vacuum freeze dried nanoparticles was found to have less thixotropic behavior compared to the suspension containing spray dried nanoparticles. The vacuum freeze dried nanoparticles can produce suspension having stronger elastic structure compared to the nanoparticles obtained from spray drying. On the other hand, the spray dried starch nanoparticles possessed more stiffness, shorter relaxation time, less irrecoverable creep deformation and higher recovery rate compared to the vacuum freeze dried nanoparticles. These rheological properties of suspension containing starch nanoparticles can contribute to the application of starch nanoparticles in drug carrying and releasing. And under different shear rate, temperature, frequency and stress, the interaction and structure variation of starch nanoparticles in suspension is still desired to be observed.

Acknowledgments

This research was supported by National Natural Science Foundation of China (31000813), Chinese Universities Scientific Fund (2012QJ009), High Technology Research and Development Program of China (2011AA100802), and Commonweal Guild Agricultural Scientific Research Project of China (201003077).

References

Agnihotri, S. A., Mallikarjuna, N. N., & Aminabhavi, T. M. (2004). Recent advances on chitosan-based micro- and nanoparticles in drug delivery. *Journal of Controlled Release*, *100*, 5–28.

Arora, A., & Padua, G. W. (2010). Review: Nanocomposites in food packaging. *Concise Reviews and Hypotheses in Food Science*, *75*(1), 43–49.

Bodnar, M., Hartmann, J. F., & Borbely, J. (2006). Synthesis and study of cross-linked chitosan-N-poly(ethylene glycol) nanoparticles. *Biomacromolecules*, *7*, 3030–3036.

Borin, D., Zubarev, A., Chirikov, D., Müller, R., & Odenbach, S. (2011). Ferrofluid with clustered iron nanoparticles: Slow relaxation of rheological properties under joint action of shear flow and magnetic field. *Journal of Magnetism and Magnetic Materials*, *323*, 1273–1277.

Cai, K.-P., Sun, J.-B., Li, Q., Wang, R., Li, B., & Zhou, J. (2011). Direct-writing construction of layered meshes from nanoparticles–vaseline composite inks: Rheological properties and structures. *Applied Physics A: Materials Science and Processing*, *102*, 501–507.

Chevalier, J., Tillement, O., & Ayela1, F. (2009). Structure and rheology of SiO_2 nanoparticle suspensions under very high shear rates. *Physical Review*, E80.

Chung, H.-J., Min, D., Kim, J.-Y., & Lim, S.-T. (2007). Effect of minor addition of xanthan on cross-linking of rice starches by dry heating with phosphate salts. *Journal of Applied Polymer Science*, *105*, 2280–2286.

Day, L., Xu, M., Øiseth, S. K., Lundin, L., & Hemar, Y. (2010). Dynamic rheological properties of plant cell-wall particle dispersions. *Colloids and Surfaces B: Biointerfaces*, *81*, 461–467.

Jain, A. K., Khar, R. K., Ahmed, F. J., & Diwan, P. V. (2008). Effective insulin delivery using starch nanoparticles as a potential trans-nasal mucoadhesive carrier. *European Journal of Pharmaceutics and Biopharmaceutics*, *69*, 426–435.

Jia, Y., Peng, K., Gong, X.-L., & Zhang, Z. (2011). Creep and recovery of polypropylene/carbon nanotube composites. *International Journal of Plasticity*, *27*(8), 1239–1251.

Kho, K., & Hadinoto, K. (2010). Aqueous re-dispersibility characterization of spray-dried hollow spherical silica nano-aggregates. *Powder Technology*, *198*, 354–363.

Kimura, H., Sakurai, M., Sugiyama, T., Tsuchida, A., Okubo, T., & Masuko, T. (2011). Dispersion state and rheology of hectorite particles in water over a broad range of salt and particle concentrations. *Rheologica Acta*, *50*, 159–168.

Kumari, K., & Rani, U. (2011). Controlled release of Metformin hydrochloride through crosslinked blends of chitosan–starch. *Advances in Applied Science Research*, *2*(2), 48–54.

Li, J., & Huang, Q.-R. (2012). Rheological properties of chitosan–tripolyphosphate complexes: From suspensions to microgels. *Carbohydrate Polymers*, *87*, 1670–1677.

Liu, D.-G., Wu, Q.-L., Chen, H.-H., & Chang, P.-R. (2009). Transitional properties of starch colloid with particle size reduction from microto nanometer. *Journal of Colloid and Interface Science*, *339*, 117–124.

Ma, X.-F., Jian, R.-J., Chang, P.-R., & Yu, J.-G. (2008). Fabrication and characterization of citric acid-modified starch nanoparticles/plasticized-starch composites. *Biomacromolecules*, *9*, 3314–3320.

Malam, Y., Lim, E. J., & Seifalian, A. M. (2011). Current trends in the application of nanoparticles in drug delivery. *Current Medicinal Chemistry*, *18*, 1067–1078.

Maroda, M., Bodnár, M., Berkó, S., Bakó, J., Erős, G., Csányi, E., et al. (2011). Preparation and investigation of a cross-linked hyaluronan nanoparticles system. *Carbohydrate Polymers*, *83*, 1322–1329.

Mcclements, D. J., Decker, E. A., & Weiss, J. (2007). Emulsion-based delivery systems for lipophilic bioactive components. *Concise Reviews/Hypotheses in Food Science*, *72*(8), 109–124.

Mohanraj, V. J., & Chen, Y. (2006). Nanoparticles – A review. *Tropical Journal of Pharmaceutical Research*, *5*(1), 561–573.

Patil, V. V., Dandekar, P. P., Patravale, V. B., & Thorat, B. N. (2010). Freeze drying: Potential for powdered nanoparticulate product. *Drying Technology*, *28*(5), 624–635.

Rodrigues, A., & Emeje, M. (2012). Recent applications of starch derivatives in nanodrug delivery. *Carbohydrate Polymers*, *87*, 987–994.

Rodríguez-Marín, M. L., Núñez-Santiago, C., Wang, Y.-J., & Bello-Pé rez, L. A. (2010). Physicochemical and structural characteristics of cross-linked banana starch using three cross-linking reagents. *Starch/Stärke*, *62*, 530–537.

Santander-Ortega, M. J., Stauner, T., Loretz, B., Ortega-Vinuesa, J. L., Bastos-González, D., Wenz, G., et al. (2010). Nanoparticles made from novel starch derivatives for transdermal drug delivery. *Journal of Controlled Release*, *141*, 85–92.

Shi, A.-M., Li, D., Wang, L.-J., Li, B.-Z., & Adhikari, B. (2011). Preparation of starch-based nanoparticles through high-pressure homogenization and miniemulsion cross-linking: Influence of various process parameters on particle size and stability. *Carbohydrate Polymers*, *83*(4), 1604–1610.

Shi, A.-M., Wang, L.-J., Li, D., & Adhikari, B. (2012). The effect of annealing and cryoprotectants on the properties of vacuum-freeze dried starch nanoparticles. *Carbohydrate Polymers*, *88*(4), 1334–1341.

Simi, C. K., & Emilia Abraham, T. (2007). Hydrophobic grafted and cross-linked starch nanoparticles for drug delivery. *Bioprocess and Biosystems Engineering*, *30*, 173–180.

Susan-Resiga, D., Bica, D., & Vékás, L. (2010). Flow behaviour of extremely bidisperse magnetizable fluids. *Journal of Magnetism and Magnetic Materials*, *322*(20), 3166–3172.

Triebel, C., & Münstedt, H. (2011). Temperature dependence of rheological properties of poly(methyl methacrylate) filled with silica nanoparticles. *Polymer*, *52*, 1596–1602.

Vigneshwaran, N., Nachane, R. P., Balasubramanya, R. H., & Varadarajan, P. V. (2006). A novel one-pot 'green' synthesis of stable silver nanoparticles using soluble starch. *Carbohydrate Research*, *341*(12), 2012–2018.

Wang, X.-H., Liu, J.-F., & Pope, M. T. (2003). New polyoxometalate/starch nanomaterial: Synthesis, characterization and antitumoral activity. *Dalton Transactions*, *5*, 957–960.

Wang, Y., Wang, L.-J., Li, D., Xue, J., & Mao, Z.-H. (2009). Effects of drying methods on rheological properties of flaxseed gum. *Carbohydrate Polymers*, *78*(2), 213–219.

Xiao, S.-Y., Liu, X.-M., Tong, C.-Y., Liu, J., Tang, D.-Y., & Zhao, L.-J. (2005). Studies of poly-L-lysine-starch nanoparticle preparation and its application as gene carrier. *Science in China Series B: Chemistry*, *48*(2), 162–166.